APSB
Acta Pharmaceutica Sinica B
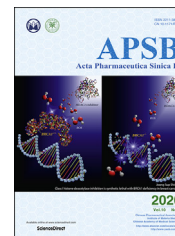
ORIGINAL ARTICLE

De novo biosynthesis of liquiritin in Saccharomyces cerevisiae

Yan Yin[a,b,†], Yanpeng Li[a,d,†], Dan Jiang[a], Xianan Zhang[b], Wei Gao[b,c,*], Chunsheng Liu[a,*]

[a]School of Chinese Pharmacy, Beijing University of Chinese Medicine, Beijing 102488, China
[b]School of Traditional Chinese Medicine, Capital Medical University, Beijing 100069, China
[c]School of Pharmaceutical Sciences, Advanced Innovation Center for Human Brain Protection, Capital Medical University, Beijing 100069, China
[d]Pharmacy Department, Beijing Longfu Hospital, Beijing 100010, China

Abstract   Liquiritigenin (LG), isoliquiritigenin (Iso-LG), together with their respective glycoside derivatives liquiritin (LN) and isoliquiritin (Iso-LN), are the main active flavonoids of *Glycyrrhiza uralensis*, which is arguably the most widely used medicinal plant with enormous demand on the market, including Chinese medicine prescriptions, preparations, health care products and even food. Pharmacological studies have shown that these ingredients have broad medicinal value, including anti-cancer and anti-inflammatory effects. Although the biosynthetic pathway of glycyrrhizin, a triterpenoid component from *G. uralensis*, has been fully analyzed, little attention has been paid to the biosynthesis of the flavonoids of this plant. To obtain the enzyme-coding genes responsible for the biosynthesis of LN, analysis and screening were carried out by combining genome and comparative transcriptome database searches of *G. uralensis* and homologous genes of known flavonoid biosynthesis pathways. The catalytic functions of candidate genes were determined by *in vitro* or *in vivo* characterization. This work characterized the complete biosynthetic pathway of LN and achieved the *de novo* biosynthesis of liquiritin in *Saccharomyces cerevisiae* using endogenous yeast metabolites as precursors and cofactors for the first time, which provides a possibility for the economical and sustainable production and application of *G. uralensis* flavonoids through synthetic biology.

1. Introduction

As an ancient botanical drug with thousands of years of history, licorice root (Glycyrrhizae Radix et Rhizoma, Gan Cao in Chinese) is a widely used medicine mainly derived from the rare and endangered herb *Glycyrrhiza uralensis* Fisch. It shows preventive and therapeutic effects against a variety of diseases with high safety, and appears in almost all Chinese medicine prescriptions, additional health care products, and even food[1,2]. In addition to triterpenoids such as glycyrrhizin, *G. uralensis* also contains a large group of flavonoids with strong biological activity[3]. The flavonoids include liquiritigenin (LG), and isoliquiritigenin (Iso-LG), as well as their respective glycoside derivatives liquiritin (LN) and isoliquiritin (Iso-LN). Iso-LG is a chalcone with high content in *G. uralensis*, and also a common natural pigment. In spite of its simple structure, Iso-LG has many significant pharmacological activities such as antiinflammatory[4], anticancer[5,6], antihistamine[7], antioxidation[8], antiplatelet agglutination[9], antiallergy[10], antivirus[11] and estrogen-like activities[12]. Its glycoside derivative Iso-LN is capable of inhibiting tumor angiogenesis[13], as well as showing antidepressant effects[14]. LG is a dihydroflavone compound formed by the isomerization of Iso-LG, which can inhibit the proliferation of certain cancer cells and induce apoptosis[15-17]. Its glycoside derivative LN is the quality indicator component of licorice root as prescribed in Chinese Pharmacopoeia. In addition to inducing apoptosis and autophagy in gastric cancer cells[18], LN can also fight depression[14]. These observations indicate that *G. uralensis* has good development and application prospects in the treatment of cancer and other diseases. Along with the attention of the cosmetics industry in search of additives from natural sources, it was found that flavonoids in *G. uralensis*, especially the above-mentioned components, can be used for the removal of reactive oxygen species (ROS), as well as the safe and gentle whitening of human skin, and as such has been used by Nivea, Shiseido, YUE-SAI cosmetics, etc[19].

Due to the enormous market demand, wild *G. uralensis* has been overharvested. Once damaged, the *G. uralensis* population is difficult to recover, and the amount of wild *G. uralensis* in China had been reduced to less than 500,000 tons as early as 2009[20]. In addition to the large reduction of *G. uralensis* production, unsustainable development also led to environmental damage and desertification in the growing area[21,22]. Coupled with the limitations of chemical synthesis and plant cell culture, sourcing the main flavonoids of *G. uralensis* through heterologous biosynthesis has become an effective strategy for the sustainable development of *G. uralensis* resources. In recent years, engineered strains have been used to produce various natural products of plant origin, including artemisinic acid[23,24], ginsenoside[25,26], paclitaxel[27], tanshinone[28], etoposide aglycone[29] and opioids[30]. As a medicinal plant of great concern, the genome of *G. uralensis* has been sequenced and published[31], and the biosynthesis pathway of the triterpenoid glycyrrhizin has been fully analyzed[32-35]. However,

the biosynthesis of LN has rarely been investigated, even though it is the main active flavonoid component in *G. uralensis*.

In this study, the key enzyme-coding genes responsible for LN biosynthesis, starting from phenylalanine ammonia-lyase, were screened out by combined genome and transcriptome analysis of *G. uralensis* and known homologous genes in the flavonoid biosynthesis pathway. The obtained LN pathway was reconstructed in yeast to realize the heterologous synthesis of the main flavonoids of *G. uralensis*, including LG, Iso-LG, LN, and Iso-LN, which provides a new method for the production and sustainable utilization of *G. uralensis* flavonoids.

2. Materials and methods

2.1. Plant materials and stress treatment

Seeds of *G. uralensis* Fisch., collected in Gansu province, were identified by Prof. Chunsheng Liu (Beijing University of Chinese Medicine, Beijing, China). The seeds were immersed in concentrated sulfuric acid for 70 min, then washed with deionized water and soaked at room temperature for 24 h. The treated seeds were sown in vermiculite and grown for 30 days in an artificial climate box (25 °C, cycles of 16 h light:8 h dark). After treatment with 0.5% NaCl or 100 mmol/L methyl jasmonate (MeJA) for 7 days, the treated plants were washed and frozen in liquid nitrogen and stored at −80 °C.

2.2. Chemicals

All of the chemical reference substances, including liquiritigenin (CAS: 578-86-9), isoliquiritigenin (CAS: 961-29-5), isoliquiritin (CAS: 5041-81-6), liquiritin (CAS: 551-15-5), phenylalanine (CAS: 63-91-2), cinnamic acid (CAS: 140-10-3), *p*-coumaric (CAS: 501-98-4), malonyl-CoA (CAS: 108347-84-8), coumaroyl-CoA (CAS: 119785-99-8), naringenin chalcone (CAS: 73692-50-9), UDP-glucose (CAS: 28053-08-9), and NADPH (CAS: 2646-71-1), had purity >98% and were commercially available (Sigma−Aldrich, Saint Louis, MO, USA; Yuanye, Shanghai, China).

2.3. Deep Illumina sequencing and transcriptome analysis

Total RNA was extracted from three biological replicates of *G. uralensis* roots using the Plant Easy Spin RNA Miniprep Kit (BIOMIGA, San Diego, CA, USA). A cDNA library was constructed after the RNA samples were qualified by Novogene (Beijing, China), and then sequenced on an HiSeq 4000 platform (Illumina, San Diego, CA, USA). The reference genome of *G. uralensis* (http://ngs-data-archive.psc.riken.jp/Gur-genome/download.pl.)[31] was used for bioinformatic transcriptome analysis, and supplemented gene functions were comprehensively annotated based on the following databases: Nr (NCBI nonredundant protein sequences), Nt (NCBI nonredundant nucleotide

sequences), Pfam (protein families), KOG/COG (clusters of orthologous groups of proteins), SwissProt (a manually annotated and reviewed protein sequence database), KEGG (Kyoto encyclopedia of genes and genomes database), GO (gene ontology) and KO (KEGG Orthology). The abundance of unigenes was normalized using the FPKM (Fragments Per Kilobase of exon per Million mapped fragments) values.

According to the annotation, the sequences of seven candidate key functional genes in the flavonoid biosynthesis pathway, including the sequences which encoding phenylalanine ammonialyase (PAL), cinnamate 4-hydroxylase (C4H), 4-coumarate CoA ligase (4CL), chalcone synthase (CHS), chalcone reductase (CHR), chalcone isomerase (CHI) and isoflavonoid 7-*O*-glycosyltransferase (F7GT/UGT), were selected. The homologous sequences of candidate genes were searched against the NCBI database and evolutionary analyses were conducted in MEGA 6.0 (Phoenix, USA)[36] by sampling 1000 bootstrap replicates. Differential gene expression analysis was performed using HemI 1.0 (Wuhan, China)[37], the abundance of candidate genes was represented by $\log_2$ values of FPKM, and sequences with $\log_2$ FPKM ≤ -1 were assigned as low expression in the samples which were excluded from the statistical data. The full-length cDNAs of the target genes were amplified by PCR using Phusion High-Fidelity PCR Master Mix (BioLabs, Ipswich, USA), and the primers designed based on the transcriptomic data (Supporting Information Table S1).

2.4. Bacterial expression and in vitro characterization

The ORFs of *PAL*, *CHS*, *CHR*, *CHI* and *UGT* were individually inserted between the *Kpn*I and *Xho*I restriction sites of pET-32a(+) using the EasyGeno Assembly Cloning kit (Tiangen, Beijing, China), and transferred into *Escherichia coli* BL21 (DE3). All primers used in vector construction are listed in Supporting Information Table S2. Transformants were screened on Luria−Bertani (LB) solid culture medium containing 100 mg/mL ampicillin and single clones were picked for sequencing verification. The recombinant cells were cultured in 200 mL of LB medium containing 100 mg/mL ampicillin at 37 °C to an OD_{600} = 0.6−1.0, after which expression was induced by isopropyl β-D-thiogalactoside (IPTG) at a final concentration of 0.2 mmol/L and continued at 16 °C for 10 h. The expressing cells were harvested by centrifugation at $8000 \times g$ and 4 °C, resuspended in 3 mL phosphate buffered solution (pH = 8.0), and disrupted by ultrasonication in an ice-bath. The crude lysate was cleared from cell debris by centrifugation at $12,000 \times g$ and 4 °C and the supernatant was collected for purification. Recombinant protein was purified using the His-Tagged Protein Purification Kit (soluble protein, CWBIO, Beijing, China), and concentrations were measured using the Enhanced BCA Protein Assay Kit (Beyotime, Shanghai, China) with BSA as the standard.

The 1 mL enzymatic reaction systems contained about 0.5 mmol/L recombinant protein (10 mmol/L phosphate buffer solution, pH = 8.0), 1 mmol/L D,L-dithiothreitol (DTT), and 1 mmol/L substrate. For CHR, an equal amount of recombinant CHS protein with known function and 1 mmol/L NADPH were added to the enzymatic system. 25 mmol/L UDP-glucose was added to the enzymatic reaction system of UGT. The reaction was incubated at 30 °C for 10 h and stopped by the addition of 200 μL methanol. The catalytic products were analyzed by HPLC−Q-TOF-MS.

2.5. Yeast expression and in vivo characterization

Cytochrome P450 gene *C4H* was expressed in *Saccharomyces cerevisiae* WAT11 using pESC-HIS as expression vector. While the catalytic product of 4CL is unstable, the candidate *4CL* and the *CHS* with known function were co-expressed in WAT11 using the binary vector pESC-LEU as expression vector. The yeast expression vector was constructed using the EasyGeno Assembly Cloning kit (Tiangen, Beijing, China). *C4H* and *CHS* were individually inserted between the *Spe*I and *Not*I sites, and *4CL* was inserted between the *Nhe*I and *Bam*HI sites of the *CHS* recombinant vector. The recombinant plasmid was transferred into WAT11 using the Frozen-EZ Yeast Transformation Kit II (Zymo Research, Los Angeles, USA), and transformants were grown on corresponding auxotrophy synthetic medium (SC-His or -Leu) with 2% glucose and 2% agar at 30 °C for 4 days. Positive clones were cultivated in the corresponding liquid auxotrophy medium (2% glucose) and shaken at 30 °C to an OD_{600} of about 0.8. The 2% glucose medium was exchanged for induction medium containing 2% galactose, and after induction at 30 °C and 220 rpm (Honour, Tianjing, China) for 6 h, 20 μmol/L cinnamic acid or coumaric acid was added and the cultivation continued for another 12 h. The fermentation broth was extracted with an equal volume of ethyl acetate three times, and after evaporation of the solvent, the products re-dissolved in methanol and analyzed by HPLC−Q-TOF-MS after passing through a 0.22 μm polytetrafluoroethylene (PTFE) filter.

2.6. HPLC−Q-TOF-MS analysis of catalytic product

The catalytic products were analyzed using an Agilent 1200 HPLC system coupled with an Agilent Q-TOF 6520 mass spectrometer (Agilent, Santa Clara, CA, USA) equipped with an electrospray ionization (ESI) device. Gradient elution was performed on an Agilent XDB-C18 column (150 mm × 2.1 mm, 3.5 μm) at room temperature with a flow rate of 0.3 mL/min using a linear gradient with water containing 0.1% formic acid (A) and acetonitrile (B) as the mobile phases as follows: 0−3 min, 5% B; 3−9 min, 25% B; 9−11 min, 25%−55% B; 11−14 min, 55%−95% B; 14−27 min, 95% B; 27−30 min, 95%−5% B. The injection volume was 20 μL.

2.7. Quantitative real-time PCR (qRT-PCR) analysis

Total RNA was extracted from roots, stems and leaves of *G. uralensis* seedlings, and reverse transcription was done used the PrimeScript™ 1st-Strand cDNA Synthesis Kit (Takara, Dalian, China) according to the manufacturer's instructions. The qRT-PCR was performed using the KAPA SYBR FAST Universal qPCR Kit (Kapa Biosystems, Boston, MA, USA) with gene-specific primer pairs (Supporting Information Table S3). Three technical replicates and three biological replicates were analyzed for each sample. The relative amounts of the target genes were evaluated based on the relative expression index of mRNA using the $2^{-\triangle\triangle Ct}$ method[38], with *Guβ-actin* as the reference gene[34].

2.8. Extraction of main flavonoids from G. uralensis

After fully pulverizing in liquid nitrogen, samples comprising about 100 mg of freeze-dried roots, stems or leaves of *G. uralensis*

seedlings that were grown for one month were accurately weighed, after which 1 mL 70% ethanol was added and the samples ultrasonically extracted at 30 °C for 30 min. The product was centrifuged, and the supernatant was passed through a 0.22 μm PTFE filter for quantitative UPLC−MS analysis.

2.9. Reconstitution of the liquiritin biosynthesis pathway in yeast and product analysis

The genes of the *G. uralensis* flavonoid pathway with known function (*GuPAL1*, *GuC4H1*, *Gu4CL1*, *GuCHS1*, *GuCHR1*, *GuCHI1*, and *GuUGT1*) were inserted in different combinations into the binary vector pESC downstream of the GAL1 or GAL10 promoters. The 3′ end of *GuCHS1* was fused to the 5′ end of *GuCHR1* via the linker sequence GGTGGTGGTTCT (*GuCHS1::GuCHR1*). The constructs were verified by bi-directional sequencing, and the resulting plasmids were used to transform the yeast strain WAT11 using the Frozen-EZ Yeast Transformation kit II (Zymo Research, Los Angeles, CA, USA). The transformants were selected on synthetic dropout plates (SC-His, -Leu, -Trp or -Ura) according to the vector label and the positive yeast clones were cultured in SC medium with 2% glucose at 30 °C and 220 rpm (Honour, Tianjing, China), and then harvested and resuspended in SC medium with 2% galactose followed by expression for 36 h. All recombinant yeast strains used in this study are listed in Supporting Information Table S4. 500 μL fermentation broth was taken and mixed with an equal volume of methanol, ultrasonicated for 60 min and centrifuged at $13,400 \times g$ for 10 min. The supernatant was analyzed by UPLC−MS after passing through a 0.22 μm PTFE filter.

2.10. Fermentation

Strain WM4-3 was used for the production of liquiritin in fed-batch fermentation. Synthetic dropout medium (SC-His-Leu-Trp-Ura) was used for both seed preparation and the fermentation. The seed culture was prepared by inoculating a 250 mL flask containing 100 mL culture medium with 2% glucose. The cells were grown at 30 °C and 250 rpm (Honour, Tianjing, China) for 48 h, and then transferred into 1 L of fresh seed medium and incubated at 30 °C and 220 rpm (Honour, Tianjing, China) for 36 h. The resulting seed was harvested and used to inoculate an 11-L New Brunswick™ BioFlo®/CelliGen® 115 fermenter (Eppendorf, Hamburg, Germany) containing 6 L of induction medium (SC-His-Leu-Trp-Ura with 2% galactose) to an initial $OD_{600} = 1.5−2.0$. The fermentation was carried out at 30 °C. The dissolved oxygen concentration (DOC) was kept above 40% and the pH was controlled at 5.0 using automatic addition of ammonium hydroxide. Concentrated synthetic dropout medium (SC-His-Leu-Trp-Ura; 80 g/L total solids) and 40% galactose were automatically fed to the fermenter separately at a rate of 6.25 mL/h from the second day. The fermentation broth was sampled at intervals of 24 h to measure the OD_{600}, and an aliquot of 500 μL volume was mixed with an equal volume of methanol, ultrasonicated for 60 min, centrifuged at $13,400 \times g$ for 10 min, and the supernatant was stored at −20 °C until UPLC−MS analysis.

2.11. Quantitative UPLC−MS analysis

The separation of 1 μL filtrate was performed using an Agilent ZORBAX RRHD SB-C18 column (100 mm × 2.1 mm, 1.8 μm) on an Agilent 1290 Infinity UPLC system (Agilent, Santa Clara, CA, USA) by gradient elution with a mobile phase comprising 0.1% (v/v) formic acid aqueous solution (A) and acetonitrile (B) at a flow rate of 0.3 mL/min. The gradient program was as follows: 0−1.0 min, 25% B; 1.0−4.0 min, 25%−90% B; 4.0−4.5 min, 90% B; 4.5−4.51 min, 90%−25% B; 4.51−5.5 min, 25%. The column temperature was set at 25 °C.

The analyte was quantified using an AB Sciex LC−MS/MS Qtrap 6500 mass spectrometer equipped with an electro-spray ionization (ESI) source (AB Sciex, Singapore). The multiple re-action monitoring (MRM) scan type was used in the negative scan mode to increase the specificity of the analysis. The mass parameters are listed in Table 1. The software MultiQuant 3.0.1 (AB Sciex, Singapore) was used to perform the data analysis.

2.12. Accession numbers

Sequence data from this article can be found in the GenBank database under the following accession numbers: *GuPAL1* (MK341789), *GuC4H1* (MK341785), *Gu4CL1* (MK341782), *GuCHS1* (MK341787), *GuCHR1* (MK341786), *GuCHI1* (MK348532), *GuUGT1* (MK341792); the transcriptome datasets: Gu-CK, SRR8400027; Gu-NaCl, SRR8400026; Gu-MeJA, SRR8468083.

3. Results

3.1. Screening of liquiritin pathway genes

Water deficiency can increase the yield of LN in the roots of *G. uralensis*[39], and MeJA is also believed to increase the production of flavonoids[40]. Consequently, deep sequencing of the *G. uralensis* root transcriptome was performed after NaCl- and MeJA-treatment, respectively (Supporting Information Tables S5 and S6). The reference genome of *G. uralensis* was used in combination with the Nr, Nt, Pfam, KOG/COG, SwissProt, KO and GO databases for bioinformatics analysis, and gene functions were comprehensively annotated, and a total of 61 genes that were annotated to encode the seven enzymes required for the biosynthesis of LN were screened from the transcriptome database (Supporting Information Table S7). Hierarchical cluster analysis of the candidate genes revealed that *GuPAL1*, *GuC4H1*, *GuCHS1*, *GuCHR1*, *GuCHR4, GuCHI1, GuCHI5* and *GuUGT1* had relatively high expression levels in both NaCl- or MeJA-treated and control *G. uralensis*. Furthermore, the treatment, and especially NaCl stress, increased the expression levels of these genes to some

Table 1 MS parameters for the quantification of analytes.

Component	Q1 Mass (Da)	Q3 Mass (Da)	Declustering potential (V)	Collision energy (V)
p-Coumaric acid	163	119	−60	−23
		93	−60	−40
Isoliquiritigenin	255	135	−80	−21
		119	−80	−30
Isoliquiritin	417	255	−180	−25
		135	−180	−30
Liquiritigenin	255	119	−100	−25
		135	−100	−20
Liquiritin	417	255	−70	−27
		135	−70	−40

extent. The expression level of *Gu4CL1* under NaCl stress was significantly higher than under MeJA stress or in the CK group (Fig. 1). In addition, multiple sequence alignment results showed that GuPAL1, GuC4H1, Gu4CL1, and GuCHS1 were respectively 78%, 92%, 72%, and 85% identical to *Populus* hybrid (*P. trichocarpa* × *P. deltoides*) PAL[41], *Glycine max* C4H[41], *Petroslinum crispum* 4CL-2[42,43], and *P.* hybrid (*P. trichocarpa* × *P. deltoides*) CHS1[42−44], which were commonly used for heterologous synthesis of plant-specific flavones.

Subsequently, to screen for the unique CHR and CHI, BLASTX analysis was performed using the NCBI database with the nucleic acid sequences that were annotated as encoding chalcone reductase (or NAD(P)H-dependent 6′-deoxychalcone synthase) and chalcone isomerase, respectively. The sequences with higher identity were used for the neighbor-joining tree
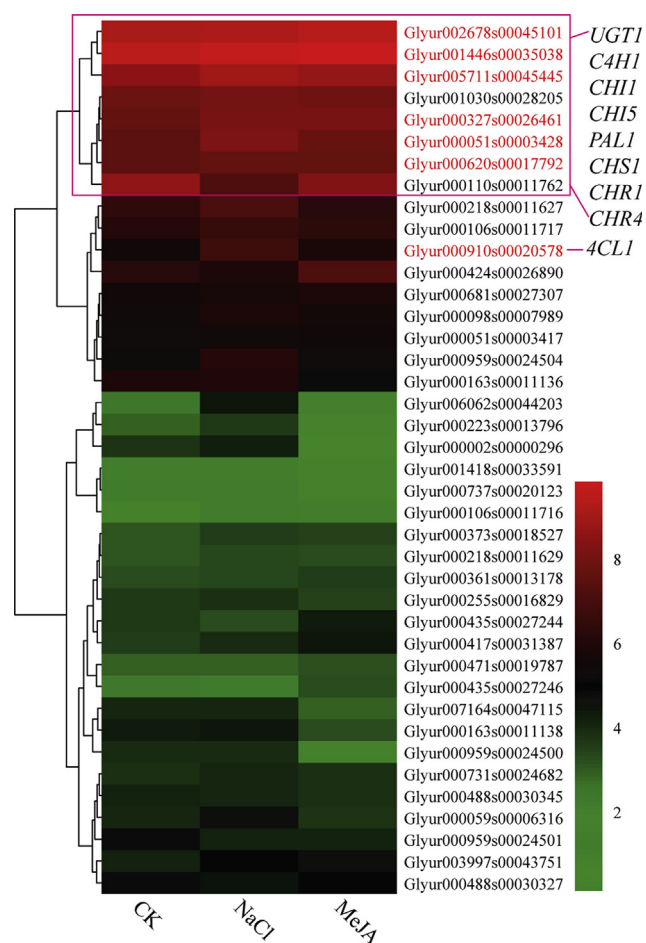

Figure 1 Hierarchical clustering and corresponding heatmaps of the differentially expressed unigenes across the flavonoid biosynthesis pathway. CK, control; NaCl, root sample treated with 0.5% NaCl; MeJA, root sample treated with 100 mmol/L MeJA. The heatmap was drawn using HemI 1.0 with $\log_2$ values of FPKM (Fragments Per Kilobase of exon per Million mapped fragments) of the candidate genes, and the sequences with $\log_2$FKPM≤−1 were assigned as low expression in the samples which were excluded from the statistical data. Depths of color in the red and green rectangles indicate higher and lower Z-scores ($\log_2$) of the corresponding RNA expression levels. The red font indicates the sequences used for liquiritin pathway reconstruction in yeast.

construction. Four *CHR* candidate genes were divided into three subgroups in the neighbor-joining tree (Fig. 2A) with GuCHR1, GuCHR2, GuCHR3 belonging to subgroup A, wherein GuCHR1 shares 87% identity to *G. max* CHR5, which had the closest correlation with the accumulation of abundant 5-deoxyisoflavonoids in soybean root[45]. GuCHR4, which is also highly expressed in *G. uralensis*, was clustered in subgroup B with *G. max* CHR4, which previous studies suggested to have no CHR activity for the production of Iso-LG[45]. The eight CHI homologs from *G. uralensis* were classified into four CHI types, whereby GuCHI1 belonged to type II CHIs, which were thought to have the activity of isomerizing Iso-LG into LG[46,47], whereas GuCHI5 fell into the type IV subfamily (Fig. 2B).

3.2. Functional characterization of liquiritin pathway enzymes

In order to confirm the catalytic function of the enzymes encoded by the candidate genes, *GuPAL1*, *GuCHS1*, *GuCHR1*, *GuCHI1* and *GuUGT1* were expressed in *E. coli* and the recombinant proteins were extracted and purified (Supporting Information Fig. S1) for *in vitro* enzymatic experiments, while the cytochrome P450 *GuC4H1* was expressed in *S. cerevisiae* WAT11. As indicated by LC−MS, incubation of the staring substrate phenylalanine with GuPAL1 yielded cinnamic acid (Fig. 3B). Similarly, the recombinant yeast harboring *GuC4H1* was able to produce *p*-coumaric acid upon feeding cinnamic acid and galactose (Fig. 3C). In an *in vitro* enzymatic system with coumaroyl-CoA and malonyl-CoA as substrates at a molar ratio of 1:3, naringenin chalcone was produced when only GuCHS1 was added. When the same amount of recombinant GuCHS1 and GuCHR1 proteins and a high concentration of NADPH (1 mmol/L) was added, the production of Iso-LG was also detected in addition to naringenin chalcone (Fig. 3E). As the catalytic product of 4CL was unstable, Gu4CL1 and GuCHS1 were co-expressed in WAT11 using the binary plasmid pESC-LEU as yeast expression vector. Upon feeding with *p*-coumaric acid, naringenin chalcone could also be detected in the culture extracts (Fig. 3D). GuCHI1, which belongs to type II CHIs, was able to isomerize Iso-LG into LG in *in vitro* enzymatic experiments, demonstrating its CHI activity (Fig. 3F). Thus, GuPAL1, GuC4H1, Gu4CL1, GuCHS1, GuCHR1 and GuCHI1 formed a complete biosynthetic pathway of liquiritigenin with phenylalanine as the precursor (Fig. 3A).

In the final step of LN biosynthesis, GuUGT1 was able to produce LN from LG *in vitro* with UDP-glucose as sugar donor (Fig. 3G). The kinetic parameters of GuUGT1, GuUGT2 and GuUGT3, respectively belong to UGT88E, UGT88H and UGT88A subfamilies within the UGT88 family (Supporting Information Fig. S2), were subsequently determined. Not surprisingly, GuUGT1 (K_m 68.17 μmol/L and V_{max} 0.87 μmol/(min·mg)) exhibited a higher maximum activity, and its catalytic efficiency (V_{max}/K_m) was also clearly higher (Supporting Information Section 1, Fig. S3 and Table S8). To investigate the structural basis for the binding of LG and UDP-glucose, a homology model was generated for GuUGT1 using the crystal structure of *Arabidopsis thaliana* UGT (PDB ID: 2VCE) with 34% identity as template (Supporting Information Section 2 and Fig. S4)[48]. The key residues of *GuUGT*1 for liquiritigenin glycosylation (Gly-14 and Gly-277) predicted by molecular docking (Supporting Information Section 3, Tables S9, S10 and Fig. S5) and residue scanning based on simulated mutations (Supporting Information Section 4 and Table S11) were different from those of the known flavonoid glucosyltransferase VvGT1 (His-20 and Asp-119) or isoflavonoid 7-*O*-
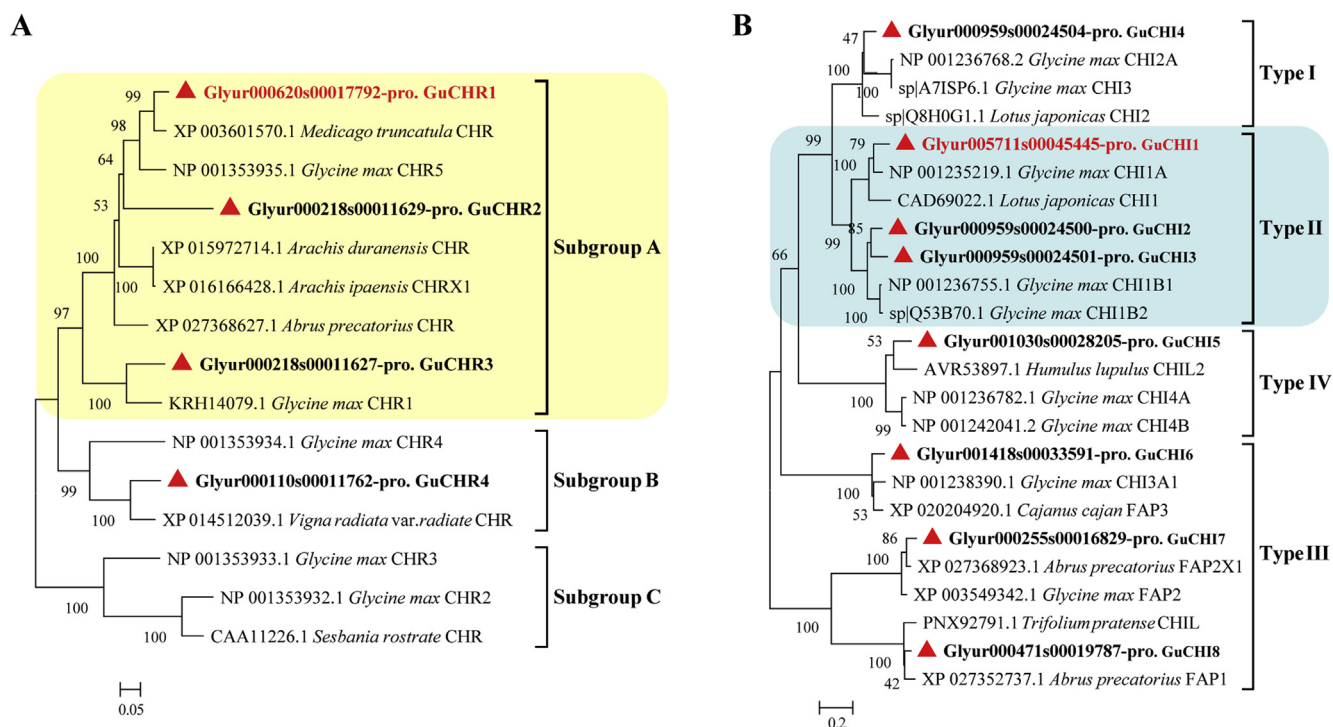
A

B

Figure 2 Phylogenetic analysis of the amino acid sequences of CHR and CHI based on the *G. uralensis* transcriptome. The evolutionary analyses were conducted in MEGA6.0 using the neighbor-joining method, and the percentage of replicate trees in which the associated taxa clustered together among the 1000 replicates in the bootstrap test are shown next to the branches. Sequences from the transcriptome were marked with red triangles. Red font indicates the sequences used for liquiritin pathway reconstruction in yeast.

glycosyltransferase GmIF7GT (Glu-392), which also belong to the UGT88E subfamily.

A comparison was made between the expression profiles of the enzymes whose catalytic functions and flavonoid accumulation in different tissues of *G. uralensis* were characterized. A pattern emerged that indicated that most LN pathway genes were mainly expressed in leaves, except for the last UGT responsible for glycosylation, which had the highest relative expression level in the roots (Fig. 3A). However, LG and Iso-LG, as well as their respective glycosylation products LN and Iso-LN are mainly accumulated in the roots (Supporting Information Fig. S6). We therefore inferred that the upstream step of LN synthesis in *G. uralensis* is mainly carried out in the leaves, and aglycones are transferred from the leaves to the roots, followed by glycosylation to form glycosides and accumulation in the roots.

3.3.   Heterologous production of G. uralensis flavonoids in yeast

Having demonstrated the catalytic abilities of all the key enzymes in the *G. uralensis* flavonoid biosynthesis pathway *in vitro* or *in vivo*, we attempted to reconstruct the main flavonoid pathway in yeast (Fig. 4A). When *GuPAL1* and *GuC4H1* were simultaneously introduced into *S. cerevisiae* WAT11, harboring the *A. thaliana* NADPH-cytochrome P450 reductase *ATR1*[49], which provides the reducing equivalents essential for the activity of plant CYP450s such as C4H, the obtained recombinant yeast WM1 was able to produce *p*-coumaric acid under galactose induction (Fig. 4B), and the content of coumaric acid reached 7.59 μmol/L after cultivation for 36 h (Fig. 4C). When the vector carrying *Gu4CL1* and *GuCHS1::GuCHR1* was transferred into

WM1, a small amount of Iso-LG was detected in the fermentation broth (Fig. 4B, WM2-1). Interestingly, Iso-LG was not detected when *GuCHS1* and *GuCHR1* were co-expressed in yeast that was fed with the substrate. After *GuCHI1* and *GuUGT1* were successively transferred to WM2-1, strains WM3-1 and WM4-1 with the capacity to produce LG and LN were respectively obtained (Fig. 4B). Compared with LN, more Iso-LG in WM4-1 was glycosylated before isomerization, resulting in 4.7 times higher Iso-LN production than that of LN in shake flasks (Fig. 4E).

3.4.   Promoting the production of flavonoids by gene overexpression

To promote the transformation of the upstream metabolites to the downstream flavonoid structure along the liquiritin pathway, we tried to overexpresses the key genes for Iso-LG biosynthesis in the described recombinant strains. The results showed that overexpression of *GuCHS1::GuCHR1* significantly increased the synthesis of Iso-LG, and the production of Iso-LG by WM2-2 was increased 18 times compared with WM2-1 (Fig. 4C). To solve the problem of the much lower production of the target product LN than Iso-LN in WM4-1, *GuCHI1* was overexpressed in WM3-1 and WM4-1, after which the yield of LG and LN increased 1.3-fold (Fig. 4D, WM3-2) and 2.1-fold (Fig. 4E, WM4-2), respectively. Moreover, simultaneous overexpression of *GuCHS1::GuCHR1* and *GuCHI1* increased the LG production of WM3-3 5.3-fold compared with WM3-1 (Fig. 4D), and the accumulation of LN in WM4-3 was 6.4 times higher than in WM4-1 (Fig. 4E). In addition, it was found that overexpression of both *GuCHI1* and *GuCHS1::GuCHR1* in this yeast system not
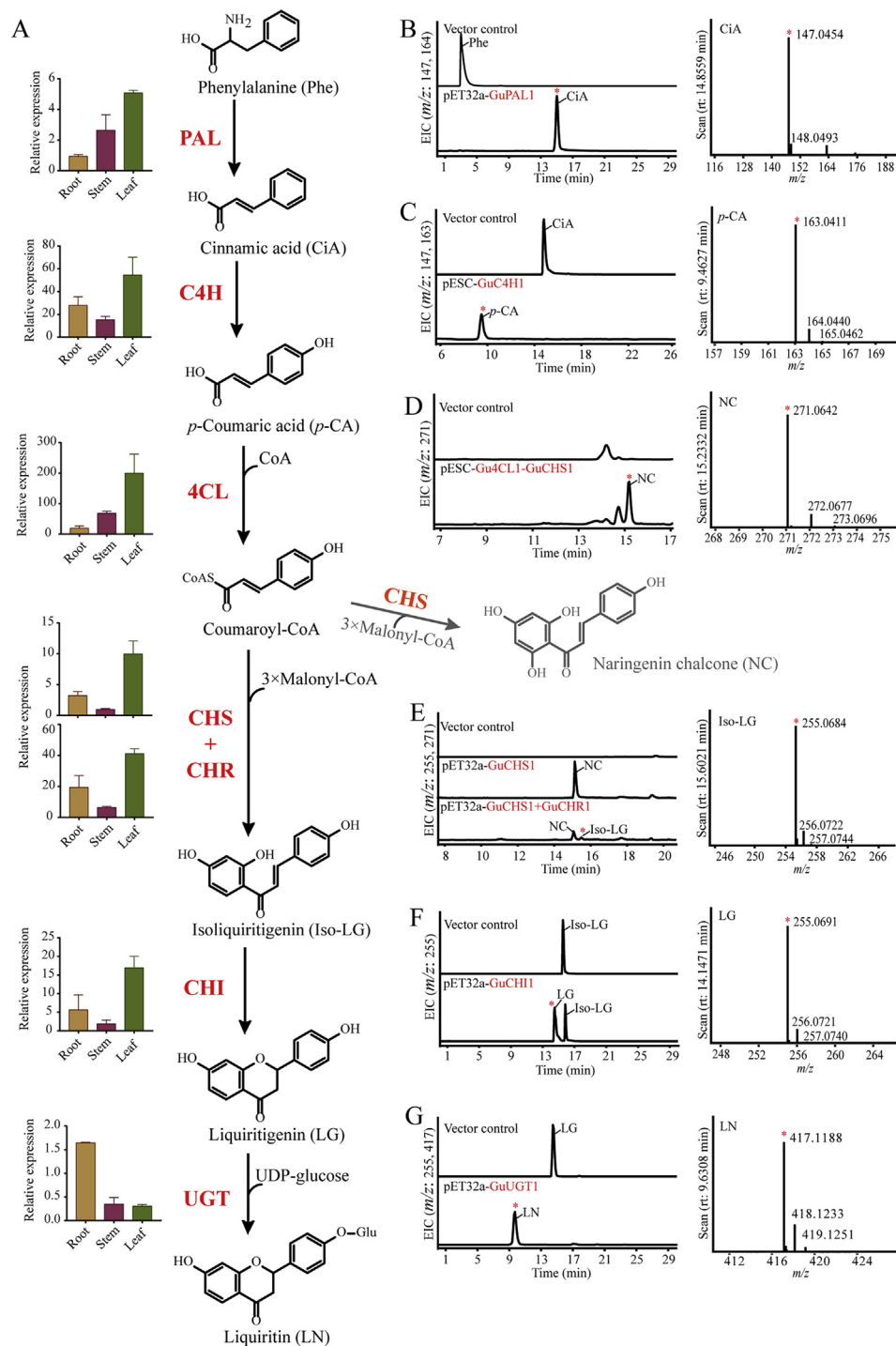
Figure 3   Analysis of catalytic products of the enzymes encoded by the candidate genes. (A) The liquiritin biosynthesis pathway of *G. uralensis*, the histogram next to each pathway enzyme name shows relative expression levels of the encoding gene (*GuPAL1*, *GuC4H1*, *Gu4CL1*, *GuCHS1*, *GuCHR1*, *GuCHI1* and *GuUGT1*) in roots, stems and leaves of *G. uralensis* determined by qRT-PCR; (B, E-G) HPLC−Q-TOF-MS profiles of the *in vitro* enzymatic products of recombinant GuPAL1 (B, phenylalanine (Phe) as substrate), GuCHS1 and GuCHR1 (E, coumaroyl-CoA as substrate), GuCHI1 (F, isoliquiritigenin (Iso-LG) as a substrate), GuUGT1 (G, liquiritigenin (LG) as a substrate) expressed in *E. coli* using pET-32a(+) as expression vector; (C, D) HPLC−Q-TOF-MS profiles of the fermentation products of yeast harboring the recombinant vector pESC-GuC4H1 (C, cinnamic acid (CiA) as a substrate) or pESC-Gu4CL1-GuCHS1 (D, *p*-coumaric acid (*p*-CA) as substrate) with external precursor addition. The peaks and mass spectrum of the product indicated by the asterisk, are shown (electron ionization in negative-ion mode, [M-H]⁻). Extracted-ion chromatogram (EIC) of the analyte, as indicated, at *m/z* 147, 164 (B), *m/z* 147, 163 (C), *m/z* 271 (D), *m/z* 255, 271 (E), *m/z* 255 (F), *m/z* 255, 417 (G). All the reactions were performed with empty vector as control.
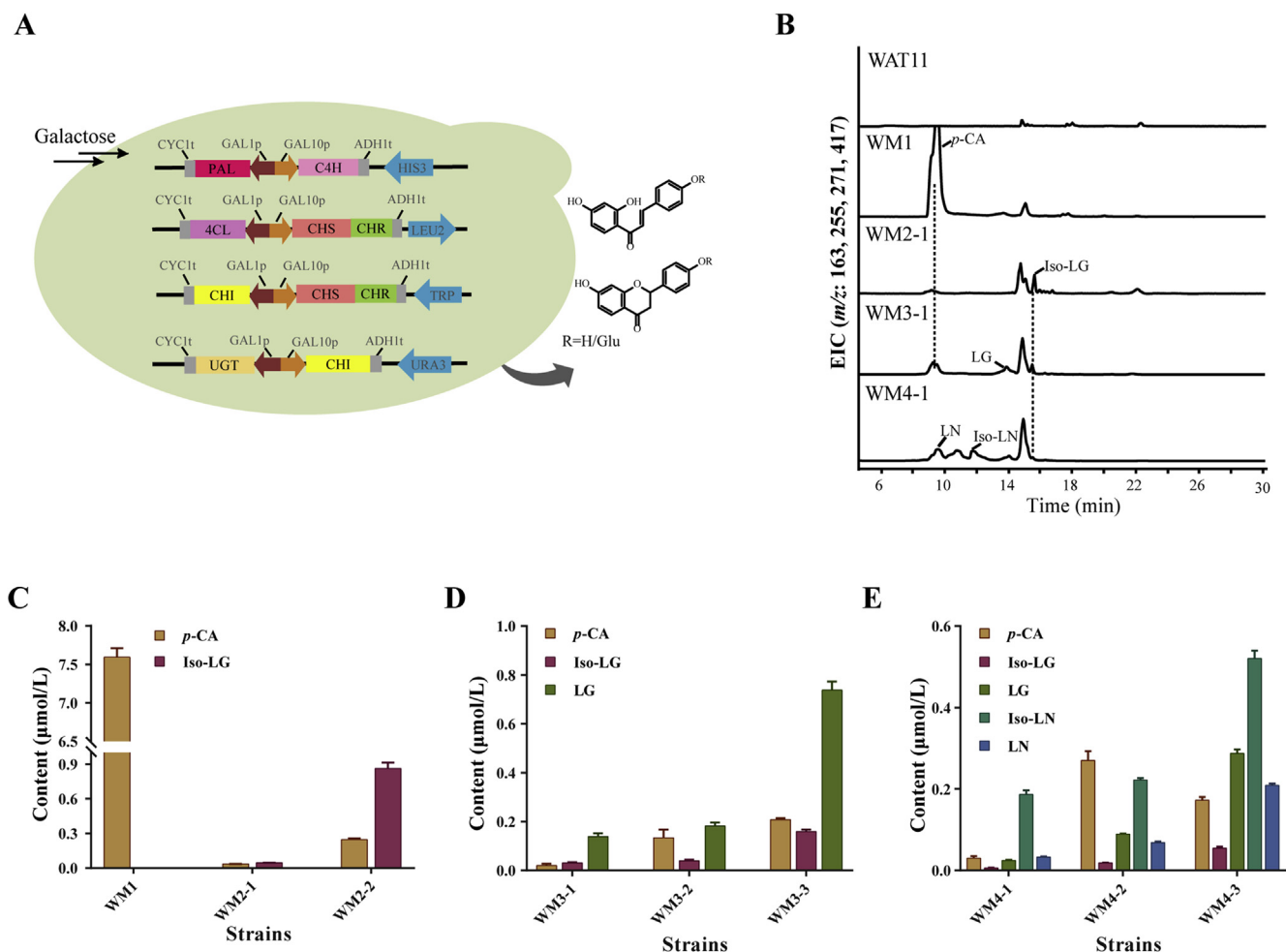
Figure 4 Reconstitution of the biosynthesis pathway of liquiritin in yeast (A) Schematic of the recombinant yeast strain WM4-1. (B) Chromatogram of selected ions with *m/z* 163, 255, 271 and 417 from the fermentation products of the recombinant yeasts using HPLC–Q-TOF-MS; (C) Production of *p*-CA and Iso-LG by yeast stains WM1 (harboring *GuPAL1*, *GuC4H1*), WM2-1 (harboring *GuPAL1*, *GuC4H1*, *Gu4CL1*, *GuCHS1*::*GuCHR1*) and WM2-2 (*GuCHS1*::*GuCHR1* overexpressed in WM2-1); (D) Production of *p*-CA, Iso-LG and LG by yeast stains WM3-1 (harboring *GuPAL1*, *GuC4H1*, *Gu4CL1*, *GuCHS1*::*GuCHR1* and *GuCHI1*), WM3-2 (*GuCHI1* overexpressed in WM3-1) and WM3-3 (*GuCHS1*::*GuCHR1* overexpressed in MW3-2) after induction with galactose for 36 h; (E) Fermentation products of yeast stains WM4-1 (harboring *GuPAL1*, *GuC4H1*, *Gu4CL1*, *GuCHS1*::*GuCHR1*, *GuCHI1* and *GuUGT1*), WM4-2 (*GuCHI1* overexpressed in WM4-1) and WM4-3 (*GuCHS1*::*GuCHR1* overexpressed in WM4-2) after induction with galactose in shake flasks. *GuCHS1*::*GuCHR1* represents a construct in which the 3′end of *GuCHS1* was fused to the 5′ end of *GuCHR1* via the linker sequence GGTGGTGGTTCT.

only increased the production of the downstream products of these enzymes, but also significantly increased the accumulation of the upstream precursor compound *p*-coumaric acid. Additionally, more glycosides (Iso-LN: 89.3%, LN: 90.3%) were secreted into the culture medium, whereas more than 30% of the Iso-LG and LG remained inside the yeast cells (Supporting Information Fig. S7).

3.5. Metabolite accumulation in the fermenter varies with the amount of cells

The changes of metabolites in the recombinant yeast strain WM4-3 with increasing induction time and biomass were also investigated in the 11 L benchtop fermenter with controlled DOC (>40%) and pH (5.0) (Fig. 5). In the early stage of fermentation, the upstream pathway accumulated a large amount of *p*-coumaric acid. Subsequently, the metabolites rapidly flowed to the final product after 24 h of fermentation, which was different from the production of a large amount of Iso-LN instead of LN observed in shake flasks (Fig. 4E). At 144 h, the accumulation of LG and LN were respectively reached 1.0 and 1.1 μmol/L. It can be seen that the fermentation conditions can greatly affect the metabolic flow direction, and the potential of this yeast fermentation system can be fully developed in the future *via* metabolic engineering and fermentation optimization.
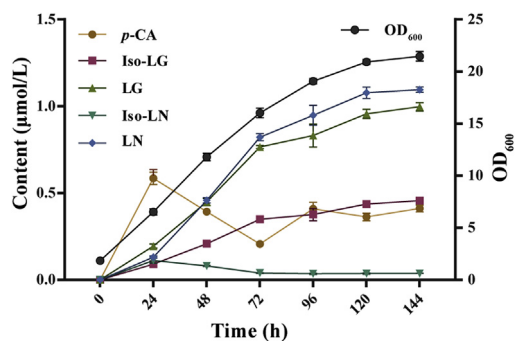
Figure 5 Cell growth and fermentation products of strain WM4-3 in fed-batch fermentation. The dissolved oxygen concentration (DOC) was kept above 40% and the pH was maintained at 5.0 using automatic addition of ammonium hydroxide. Three replicates were performed for each analysis and the error bars represented the standard deviation (SD).

4. Discussion

Flavonoids are an important class of compounds widely found in nature. In addition to their contribution to the gorgeous colors of plants, their enormous medicinal potential has become the most active area of flavonoid research in recent years[50]. With the rapid development of genetic and metabolic engineering, great progress has been made in the analysis of biosynthetic pathways of flavonoids[51]. The complete pathways of plant-specific flavonoids such as quercetin, resveratrol, kaempferol[41], scutellarin[52], baicalein and scutellarein[43] have been reconstructed in *S. cerevisiae* or *E. coli*. Some researchers have also expressed a part of the genes encoding the enzymes in the LG biosynthetic pathway from plasmids in *E. coli* or *S. cerevisiae*, and attempted to convert exogenously fed phenylpropanoid acids into 5-deoxyflavonoids such as Iso-LG and LG, but the main fermentation product they obtained was naringenin[42]. In this study, the complete biosynthetic pathway of the main flavonoid of *G. uralensis,* LN, was characterized and reconstructed in *S. cerevisiae*, and achieved the *de novo* biosynthesis of LN using raw materials and cofactors from the endogenous yeast metabolism. This provides a possibility of economically and sustainably producing *G. uralensis* flavonoids through synthetic biology.

The biosynthesis of LN is initiated *via* the general phenylpropanoid metabolism, but the downstream steps of its synthetic pathway leads to the production of 5-deoxyflavonoids (Iso-LG, LG) due to the role of CHR, which is different from the synthetic pathways of quercetin and other 5-hydroxyisoflavonoids. CHR, also known as NADPH-dependent 6′-deoxychalcone synthase, can only work with CHS at high concentrations of NADPH ($\geq$ 0.1 mmol/L) to convert malonyl-CoA and coumaroyl-CoA to synthesize Iso-LG. Otherwise, only naringenin chalcone, the catalytic product of CHS, can be generated[53]. Therefore, in the *in vitro* enzymatic reaction system of CHR, 0.1 mmol/L NADPH was added. Nevertheless, naringenin chalcone still accounted for the main part of the catalytic products in spite of the production of Iso-LG (Fig. 3E). In addition, we also used *S. cerevisiae* WAT11 as a natural NADPH supplier, in which *GuCHS1* and *GuCHR1* were co-expressed, and the precursor compound was fed during fermentation, but no Iso-LG was detected in the extract of the fermentation broth. Although studies have shown that CHR has no obvious

interaction with CHS or even other cytoplasmic enzymes in the isoflavone pathway except for IFS[45], interestingly, the recombinant yeast expressing the fusion of *GuCHS1* and *GuCHR1* was able to produce Iso-LG instead of naringenin chalcone (Fig. 4B). This is in contrast to the LG-producing strain constructed by the Mattheos research team[42], which produces more by-product, naringenin chalcone, than the target product Iso-LG. The fusion of *GuCHS1* and *GuCHR1* may play a role in shortening the time and distance that the unstable intermediates must traverse from CHS to CHR, which is similar to the immobilization of CHS and CHR recombinant proteins on Ni^{2+}-coated beads, which was reported to significantly increase the proportion of deoxygenated products[45].

In the reconstruction of the LN pathway in yeast, the overexpression of *GuCHI1* significantly increased the yield of *p*-coumaric acid in the upstream pathway even though CHIs have relatively slower kinetics in the conversion of Iso-LG to LG[54], and overexpression of *GuCHS1*::*GuCHR1* was able to significantly increase the accumulation of both upstream and downstream products (Fig. 4C−E). This phenomenon suggests that there may be an interaction between the different genes of the pathway, or that the downstream product of the LN pathway exerts a positive feedback effect on the upstream pathway. The possible mechanisms need further study.

Author contributions

Wei Gao and Chunsheng Liu designed the research. Yan Yin and Yanpeng Li performed the experiments under the guidance of Wei Gao and Chunsheng Liu. Yan Yin and Yanpeng Li finished the sketch, Dan Jiang and Xianan Zhang analyzed the data and revised the manuscript. All authors contributed a lot to this work and approved the final version of the manuscript.

Conflicts of interest

The authors have no conflicts of interest to declare.

Appendix A. Supporting information

Supporting data to this article can be found online at https://doi.org/10.1016/j.apsb.2019.07.005.

References

1. Gao X, Wang W, Wei S, Li W. Review of pharmacological effects of *Glycyrrhiza radix* and its bioactive compounds. *China J Chin Mater Med* 2009;**34**:2695−700.

2. Li T, Zhuang S, Wang Y, Wang Y, Wang W, Zhang H, et al. Flavonoid profiling of a traditional Chinese medicine formula of Huangqin Tang using high performance liquid chromatography. *Acta Pharm Sin B* 2016;**2**:148−57.

3. Wang L, Yang R, Yuan B, Liu Y, Liu C. The antiviral and antimicrobial activities of licorice, a widely-used Chinese herb. *Acta Pharm Sin B* 2015;**4**:310−5.

4. Traboulsi H, Cloutier A, Boyapelly K, Bonin MA, Marsault É, Cantin AM, et al. The flavonoid isoliquiritigenin reduces lung inflammation and mouse morbidity during influenza virus infection. *Antimicrob Agents Chemother* 2015;**59**:6317−27.

5. Kanazawa M, Satomi Y, Mizutani Y, Ukimura O, Kawauchi A, Sakai T, et al. Isoliquiritigenin inhibits the growth of prostate cancer. *Eur Urol* 2003;**43**:580−6.

6. Gao F, Zhang J, Fu C, Xie X, Peng F, You J, et al. iRGD-modified lipid-polymer hybrid nanoparticles loaded with isoliquiritigenin to enhance anti-breast cancer effect and tumor-targeting ability. *Int J Nanomed* 2017;**12**:4147−62.

7. Kim DC, Choi SY, Kim SH, Yun BS, Yoo ID, Reddy NR, et al. Isoliquiritigenin selectively inhibits H_2 histamine receptor signaling. *Mol Pharmacol* 2006;**70**:493−500.

8. Chen H, Zhang B, Yuan X, Yao Y, Zhao H, Sun X, et al. Isoliquiritigenin-induced effects on Nrf2 mediated antioxidant defence in the HL-60 cell monocytic differentiation. *Cell Biol Int* 2013;**37**:1215−24.

9. Li YY, Yang L, Chai X, Yang JJ, Wang YF, Zhu Y. Four major urinary metabolites of liquiritigenin in rats and their anti-platelet aggregation activity. *Chem Nat Compd* 2018;**54**:443−6.

10. Hou Y, Che D, Ma P, Zhao T, Zeng Y, Wang N. Anti-pseudo-allergy effect of isoliquiritigenin is MRGPRX2-dependent. *Immunol Lett* 2018;**198**:52−9.

11. Feng Yeh C, Wang KC, Chiang LC, Shieh DE, Yen MH, San Chang J. Water extract of licorice had anti-viral activity against human respiratory syncytial virus in human respiratory tract cell lines. *J Ethnopharmacol* 2013;**148**:466−73.

12. Maggiolini M, Statti G, Vivacqua A, Gabriele S, Rago V, Loizzo M, et al. Estrogenic and antiproliferative activities of isoliquiritigenin in MCF7 breast cancer cells. *J Steroid Biochem Mol Biol* 2002;**82**:315−22.

13. Liu JH, Wei HB, Yao Y, Zheng QS. Anti-tumor angiogenesis of four different active ingredients from *Glycyrrhiza*. *Prog Mod Biomed* 2010;**10**:2731−4.

14. Wang W, Hu X, Zhao Z, Liu P, Hu Y, Zhou J, et al. Antidepressant-like effects of liquiritin and isoliquiritin from *Glycyrrhiza uralensis* in the forced swimming test and tail suspension test in mice. *Prog Neuropsychopharmacol Biol Psychiatr* 2008;**32**:1179−84.

15. Xie SR, Wang Y, Liu CW, Luo K, Cai YQ. Liquiritigenin inhibits serum-induced HIF-1α and VEGF expression *via* the AKT/mTOR-p70S6K signalling pathway in heLa cells. *Phytother Res* 2012;**26**:1133−41.

16. Liu C, Wang Y, Xie S, Zhou Y, Ren X, Li X, et al. Liquiritigenin induces mitochondria-mediated apoptosis *via* cytochrome c release and caspases activation in heLa Cells. *Phytother Res* 2011;**25**:277−83.

17. Zhang SP, Zhou YJ, Liu Y, Cai YQ. Effect of liquiritigenin, a flavanone existed from Radix glycyrrhizae on pro-apoptotic in SMMC-7721 cells. *Food Chem Toxicol* 2009;**47**:693−701.

18. Wei F, Jiang X, Gao HY, Gao SH. Liquiritin induces apoptosis and autophagy in cisplatin (DDP)-resistant gastric cancer cells *in vitro* and xenograft nude mice *in vivo*. *Int J Oncol* 2017;**51**:1383−94.

19. Wang JG, Zhou Z, Liu HF, Wang JX. Application of active glycyrrhizic constituents to cosmetics. *China Surf Deter Cosmet* 2004;**34**:249−51.

20. Huang M, Wang W, Wei S. Investigation on medicinal plant resources of *Glycyrrhiza uralensis* in China and chemical assessment of its underground part. *China J Chin Mater Med* 2010;**35**:947−52.

21. Wang Q, Li J, Simayi H. Utilization status and protection measures for licorice resources in Xinjiang. *Grass-Feed Livest* 2018;**2018**:52−6.

22. Yang L, Chen J, Yang T, Li Z, Hu W, Wang Y. Geographic distribution and resource survey of the wild medicinal plants licorice (*Glycyrrhiza uralensis*) in northwest China. *Chin Wild Plant Res* 2013;**32**:27−31.

23. Ro DK, Paradise EM, Ouellet M, Fisher KJ, Newman KL, Ndungu JM, et al. Production of the antimalarial drug precursor artemisinic acid in engineered yeast. *Nature* 2006;**440**:940−3.

24. Paddon CJ, Westfall PJ, Pitera DJ, Benjamin K, Fisher K, McPhee D, et al. High-level semi-synthetic production of the potent antimalarial artemisinin. *Nature* 2013;**496**:528−32.

25. Dai Z, Wang B, Liu Y, Shi M, Wang D, Zhang X, et al. Producing aglycons of ginsenosides in bakers' yeast. *Sci Rep* 2014;**4**:3698.

26. Wang P, Wei Y, Fan Y, Liu Q, Wei W, Yang C, et al. Production of bioactive ginsenosides Rh2 and Rg3 by metabolically engineered yeasts. *Metab Eng* 2015;**29**:97−105.

27. Ajikumar PK, Xiao WH, Tyo KE, Wang Y, Simeon F, Leonard E, et al. Isoprenoid pathway optimization for Taxol precursor overproduction in *Escherichia coli*. *Science* 2010;**330**:70−4.

28. Zhou YJ, Gao W, Rong Q, Jin G, Chu H, Liu W, et al. Modular pathway engineering of diterpenoid synthases and the mevalonic acid pathway for miltiradiene production. *J Am Chem Soc* 2012;**134**:3234−41.

29. Lau W, Sattely ES. Six enzymes from mayapple that complete the biosynthetic pathway to the etoposide aglycone. *Science* 2015;**349**:1224−8.

30. Galanie S, Thodey K, Trenchard IJ, Filsinger Interrante M, Smolke CD. Complete biosynthesis of opioids in yeast. *Science* 2015;**349**:1095−100.

31. Mochida K, Sakurai T, Seki H, Yoshida T, Takahagi K, Sawai S, et al. Draft genome assembly and annotation of *Glycyrrhiza uralensis*, a medicinal legume. *Plant J* 2017;**89**:181−94.

32. Seki H, Ohyama K, Sawai S, Mizutani M, Ohnishi T, Sudo H, et al. Licorice β-amyrin 11-oxidase, a cytochrome P450 with a key role in the biosynthesis of the triterpene sweetener glycyrrhizin. *Proc Natl Acad Sci U S A* 2008;**105**:14204−9.

33. Seki H, Sawai S, Ohyama K, Mizutani M, Ohnishi T, Sudo H, et al. Triterpene functional genomics in licorice for identification of CYP72A154 involved in the biosynthesis of glycyrrhizin. *Plant Cell* 2011;**23**:4112−23.

34. Xu G, Cai W, Gao W, Liu C. A novel glucuronosyltransferase has an unprecedented ability to catalyse continuous two-step glucuronosylation of glycyrrhetinic acid to yield glycyrrhizin. *New Phytol* 2016;**212**:123−35.

35. Chen H, Liu Y, Zhang X, Zhan X, Liu C. Cloning and characterization of the gene encoding β-amyrin synthase in the glycyrrhizic acid biosynthetic pathway in *Glycyrrhiza uralensis*. *Acta Pharm Sin B* 2013;**6**:416−24.

36. Tamura K, Stecher G, Peterson D, Filipski A, Kumar S. MEGA6: molecular evolutionary genetics analysis version 6.0. *Mol Biol Evol* 2013;**30**:2725−9.

37. Deng W, Wang Y, Liu Z, Cheng H, Xue Y. HemI: a toolkit for illustrating heatmaps. *PLoS One* 2014;**9**:e111988.

38. Livak KJ, Schmittgen TD. Analysis of relative gene expression data using real-time quantitative PCR and the method. *Methods* 2001;**25**:402−8.

39. Li WD, Hou JL, Wang WQ, Tang XM, Liu CL, Xing D. Effect of water deficit on biomass production and accumulation of secondary metabolites in roots of *Glycyrrhiza uralensis*. *Russ J Plant Physiol* 2011;**58**:538−42.

40. Jeong YJ, An CH, Park SC, Pyun JW, Lee J, Kim SW, et al. Methyl jasmonate increases isoflavone production in soybean cell cultures by activating structural genes involved in isoflavonoid biosynthesis. *J Agric Food Chem* 2018;**66**:4099−105.

41. Trantas E, Panopoulos N, Ververidis F. Metabolic engineering of the complete pathway leading to heterologous biosynthesis of various flavonoids and stilbenoids in *Saccharomyces cerevisiae*. *Metab Eng* 2009;**11**:355−66.

42. Yan Y, Huang L, Koffas MA. Biosynthesis of 5-deoxyflavanones in microorganisms. *Biotechnol J* 2007;**2**:1250−62.

43. Li J, Tian C, Xia Y, Mutanda I, Wang K, Wang Y. Production of plant-specific flavones baicalein and scutellarein in an engineered *E. coli* from available phenylalanine and tyrosine. *Metab Eng* 2019;**52**:124−33.

44. Leonard E, Yan Y, Fowler ZL, Li Z, Lim CG, Lim KH, et al. Strain improvement of recombinant *Escherichia coli* for efficient production of plant flavonoids. *Mol Pharm* 2008;**5**:257−65.

45. Mameda R, Waki T, Kawai Y, Takahashi S, Nakayama T. Involvement of chalcone reductase in the soybean isoflavone metabolon: identification of GmCHR5, which interacts with 2-hydroxyisoflavanone synthase. *Plant J* 2018;**96**:56−74.

46. Ralston L, Subramanian S, Matsuno M, Yu O. Partial reconstruction of flavonoid and isoflavonoid biosynthesis in yeast using soybean type I and type II chalcone isomerases. *Plant Physiol* 2005;**137**:1375−88.

47. Ban Z, Qin H, Mitchell AJ, Liu B, Zhang F, Weng JK, et al. Non-catalytic chalcone isomerase-fold proteins in *Humulus lupulus* are auxiliary components in prenylated flavonoid biosynthesis. *Proc Natl Acad Sci U S A* 2018;**115**:E5223−32.

48. Brazier-Hicks M, Offen WA, Gershater MC, Revett TJ, Lim EK, Bowles DJ, et al. Characterization and engineering of the bifunctional *N*- and *O*-glucosyltransferase involved in xenobiotic metabolism in plants. *Proc Natl Acad Sci U S A* 2007;**104**:20238−43.

49. Urban P, Mignotte C, Kazmaier M, Delorme F, Pompon D. Cloning, yeast expression, and characterization of the coupling of two distantly related *Arabidopsis thaliana* NADPH-cytochrome P450 reductases with P450 CYP73A5. *J Biol Chem* 1997;**272**:19176−86.

50. Harborne JB, Williams CA. Advances in flavonoid research since 1992. *Phytochemistry* 2000;**55**:481−504.

51. Winkel-Shirley B. Flavonoid biosynthesis. A colorful model for genetics, biochemistry, cell biology, and biotechnology. *Plant Physiol* 2001;**126**:485−93.

52. Liu X, Cheng J, Zhang G, Ding W, Duan L, Yang J, et al. Engineering yeast for the production of breviscapine by genomic analysis and synthetic biology approaches. *Nat Commun* 2018;**9**:448.

53. Ayabe SI, Udagawa A, Furuya T. NAD(P)H-dependent 6'-deoxy-chalcone synthase activity in *Glycyrrhiza echinata* cells induced by yeast extract. *Arch Biochem Biophys* 1988;**261**:458−62.

54. Jez JM, Noel JP. Reaction mechanism of chalcone isomerase. pH dependence, diffusion control, and product binding differences. *J Biol Chem* 2002;**277**:1361−9.